

The Effect of Substitution of CaO/MgO and CaO/SrO on *in vitro* Bioactivity of Sol-Gel Derived Bioactive Glass

Zeinab Hajifathali, Moghan Amirhosseinian

Abstract—This study had two main aims: firstly, to determine how the individual substitution of CaO/MgO and CaO/SrO can affect the *in vitro* bioactivity of sol-gel derived substituted 58S bioactive glass (BG) and secondly to introduce a composition in the $60\text{SiO}_2-(36-x)\text{CaO}-4\text{P}_2\text{O}_5-(x)\text{MgO}$ and $60\text{SiO}_2-(36-x)\text{CaO}-4\text{P}_2\text{O}_5-(x)\text{SrO}$ quaternary systems (where $x=0, 5, 10$ mol.%) with enhanced biocompatibility, alkaline phosphatase (ALP) activity, and more efficient antibacterial activity against MRSA bacteria. Results showed that both magnesium-substituted bioactive glasses (M-BGs) and strontium- substituted bioactive glasses (S-BGs) retarded the Hydroxyapatite (HA) formation. Meanwhile, magnesium had more pronounced effect. The 3-(4, 5dimethylthiazol-2-yl)-2,5-diphenyltetrazolium bromide (MTT) and ALP assays revealed that the presence of moderate amount (5 mol%) of Mg and Sr had a stimulating effect on increasing of both proliferation and differentiation of MC3T3-E1 cells. Live dead and Dapi/actin staining revealed both substitution of CaO/MgO and CaO/SrO resulted in more biocompatibility and stimulation potential of the MC3T3 cells compared with control. Taken together, among all of the synthesized magnesium substituted (MBGs) and strontium substituted (SBGs), the sample 58- BG with 5 mol% CaO/MgO substitution (BG-5M) was considered as a multifunctional biomaterial in bone tissue regeneration field with enhanced biocompatibility, ALP activity as well as the highest antibacterial efficiency against methicillin-resistant *Staphylococcus aureus* (MRSA) bacteria.

Keywords—Apatite, alkaline earth, bioactivity, biomedical applications, sol-gel.

I. INTRODUCTION

BGs are silica-based synthetic biomaterials firstly discovered by Hench in $46.1\text{SiO}_2-24.4\text{Na}_2\text{O}-26.9\text{CaO}-2.6\text{P}_2\text{O}_5$ (mol%) system in the early 1970s [1]. BGs have capability of bonding directly to the surrounding living bone through the formation of a HA interface layer on their surface inside a human body [2]. Moreover, BGs are biodegradable and can stimulate the bone regeneration by the action of their dissolution products on cells [2], [3]. Hence, because of the aforementioned unique properties, they can be used as a promising biomaterials in bone tissue engineering [3], [4].

BGs can be synthesized by two different routes: conventional melt-quenching or sol-gel methods. The sol-gel technique requires considerably much lower temperature and has advantages of compositional purity compared with melt-

quenching method [5]. Sol-gel derived BGs have higher dissolution rate and followed by increased HA formation rate with respect to melt-quench derived BGs due to higher specific surface area [6]. In addition, sol-gel derived BGs also have high silanol (Si-OH) groups on their surfaces which act as active sites for further functionalization [7].

Synthesis, characterization, and biological behavior of 58S-BG (60% SiO_2 -36% CaO -4% P_2O_5 (in mol. pct.) have been reported in several studies [6], [8], [9]. Various amounts of modifier such as magnesium (Mg) [10], [11], strontium (Sr) [12], [13], zinc (Zn) [14], copper (Cu) [15], silver (Ag) [16], [17] and, lithium (Li) [18] are incorporated in BGs composition to improve their particular properties such as osteoconductivity [19], [20], angiogenicity [15] and antibacterial [21].

A bacterial infection mostly leads to a surgical failure and following second operations or removal and replacement of implanted biomaterial components [22], [23]. Therefore, prevention against bacterial infection is vital in orthopedic surgery [23]. The idea of using the BGs as antibiotic-free antibacterial biomaterials was previously mentioned [5], [24]. Moreover, BGs can prevent and reduce the risk of post-operative bacterial infections [25]. Despite recent confirmation of the antibacterial properties of the BGs [26], the exact mechanism of action is still unknown [27].

The Gram-positive methicillin-resistant *Staphylococcus aureus* (MRSA) is a type of staph bacteria that which resistant to several antibiotics [28]. Incorporation the specific metallic ions in BG's composition such as M-BG and S-BG has been investigated for the antibacterial properties [11], [22].

Magnesium, one of the alkaline earth element, is the fourth most abundant cation in the human body [29]. The most of the body's Mg (approx. 65%) is present in bone and teeth. Furthermore, on one hand, Mg plays a major role in bone metabolism and can induce new bone formation due to direct interaction with osteoblast cells which are responsible for cell adhesion and stability [30] and on the other hand, its deficiency is directly associated with osteoporosis, causing decreased bone growth and increased bone resorption [31].

Strontium (Sr), another alkaline earth element, has attracted attention like other two important divalent metals calcium and magnesium in human biology [32]. Moreover, Sr plays a similar role as calcium (Ca) in bone formation [33] and also Sr has been clinically used for treatment of osteoporosis [34], [35].

Despite some studies on the individual effect of Mg or Sr

Zeinab Hajifathali is with the Department of Materials Engineering, Imam Khomeini International University, Qazvin, 34149-16818, Iran (corresponding author, e-mail: alirajabpourikiu@gmail.com).

Moghan Amirhosseinian is with the Department of Materials Engineering, Imam Khomeini International University, Qazvin, 34149-16818, Iran.

ions on BG bioactivity, the effect of these ions on *in vitro* bioactivity has not been stated exactly up to now. On the other words, there are many controversial results were reported regarding the influence of Mg/Ca or Sr/Ca substitution on HA formation for MBGs or SBGs, respectively. For example, some claims have been reported that either Mg [36]–[39] or Sr [40]–[47] increased the BG bioactivity by reduction of the bone resorption and formation of a new bone, while the complete reverse effect of Mg [11], [48]–[50] or Sr [46], [51]–[55] on BG bioactivity was reported. Meanwhile, Moya et al. and Christi et al. respectively showed that substitution of CaO with Mg [56] or SrO [57] in BG had an insignificant effect on HA formation rate and the bioactivity remained constant. Furthermore, the optimal amount of substituted Mg/Ca or Sr/Ca in BG composition which has the highest positive effect on cell proliferation and activity has not been elucidated exactly.

TABLE I
COMPOSITIONS OF THE BG-0, M-BGS AND S-BGS (IN MOL %)

BGs	Label	SiO ₂	CaO	P ₂ O ₅	MgO	SrO
58S-0%MgO-0%SrO	BG-0	60	36	4	0	0
58S-5%MgO-0%SrO	BG-5M	60	31	4	5	0
58S-0%MgO-5%SrO	BG-5S	60	31	4	0	5
58S-10%MgO-0%SrO	BG-10M	60	26	4	10	0
58S-0%MgO-10%SrO	BG-10S	60	26	4	0	10

This study had two main aims. The first was to compare how *in vitro* bioactivity was affected by substitution of either Mg²⁺ or Sr²⁺ in place of Ca²⁺ in 58S-BG; and the second was to introduce the best candidate in the 60SiO₂–(36-x)CaO–4P₂O₅–(x)MgO and 60SiO₂–(36-x)CaO–4P₂O₅–(x)SrO quaternary systems (with x=0, 5, 10 mol%) in bone repair/regeneration, mainly in stimulating the proliferation, differentiation, ALP activity of osteoblastic MC3T3-E cells as well as the most efficient antibacterial activity against MRSA bacteria.

II. MATERIALS AND METHOD

A. Materials

Magnesium and strontium substituted 58S (60SiO₂–36CaO–4P₂O₅, mol%) were synthesized with tetraethyl orthosilicate (TEOS, Merck), triethyl phosphate (TEP, Merck), calcium nitrate tetrahydrate (Ca(NO₃)₂·4H₂O, Merck), strontium nitrate (Sr(NO₃)₂, Merck) and magnesium nitrate hexahydrate (Mg(NO₃)₂·6H₂O, Merck), using the sol–gel technique. The details of the chemical composition of the synthesized BGs used for the present study are given in Table I.

In addition, *in vitro* study was carried out in SBF solution was synthesized by using NaCl, KCl, K₂HPO₄, 3H₂O, MgCl₂·6H₂O, CaCl₂, Na₂SO₄ reagents, tris (hydroxymethyl) aminomethane (HOCH₂)₃CNH₂, and HCl based on the Kokubo's procedure as described in the literature [58].

A mouse osteoblast-like cell line (MC3T3-E1, Sigma-Aldrich), was selected for biological investigation. Cells were cultured in α -MEM supplemented with 10% fetal bovine serum (FBS), (Sigma-Aldrich, UK), 1% antibiotic, 2 mM

glutamine and 0.1% penicillin-streptomycin under standard conditions (at 37 °C in a humidified atmosphere of 95% air and 5% carbon dioxide) with a change of culture medium every other day. The confluent cells were dissociated with trypsin and subcultured to three passages were used for biological experiments.

B. BG Synthesis

TEOS, distilled water, and 0.1 M nitric acid were vigorously mixed for 1 h by a magnetic stirrer at room temperature to ensure complete hydrolysis of TEOS. Afterwards, TEP, Ca(NO₃)₂·4H₂O, and Mg(NO₃)₂·6H₂O or Sr(NO₃)₂ (for M-BGs and S-BGs, respectively) were added sequentially with time intervals of 45 min. The resultant sol then poured into Pyrex container and kept sealed at 37 °C for 3 days and followed by calcination of the dried gel in a furnace at 700 °C for 3 h to ensure elimination the nitrates and organic substances. Finally, calcined powders were compressed into tablet (\varnothing 10×3 mm) with hydraulic press under 9 MPa pressure in order to *in vitro* studies.

C. Characterization of Formed HA on Substituted BGs Surfaces

1. X-Ray Diffraction Analysis

After 7 and 14 days immersion in SBF, BG-0, MBGs and S-BGs surfaces were analyzed by X-ray diffraction (XRD, INEL-Equinox-3000, France) to investigate the HA formation on their surfaces. Instrument works with voltage of 40 kV and uses Cu-K α radiation source ($\lambda = 1.5405 \text{ \AA}$) and XRD diagrams were recorded in the interval $20^\circ \leq 2\theta \leq 50^\circ$.

2. FTIR Analysis

The BG-0, MBGs and S-BGs surfaces were performed after 7 and 14 days immersion in SBF by Fourier transform infrared spectroscopy (FTIR, Nicolet Avatar 660 (Nicolet, USA)) to investigate the HA formation on the MBGs surfaces. For this purpose, 1 mg of material scraped from MBG surface was mixed with 100 mg of KBr and palletized under vacuum. Then, the pellets were analyzed in the range of 400–4000 cm⁻¹ with a resolution of 8 cm⁻¹.

3. Inductively Coupled Plasma-Atomic Emission Spectroscopy

For *in vitro* evaluation, the disk-shaped BGs were soaked in the SBF at 37 °C for 1, 3, 7, and 14 days. The ratio of the MBG surface area to the SBF volume was approximately 0.1 cm² mL⁻¹. At the end of each time period, disk-shaped BGs were removed from the SBF and the reacted solution was analyzed. The concentrations of Ca, Si, P, Mg and Sr ions were investigated by using inductively coupled plasma atomic emission spectroscopy (ICP-AES; Varian Vista Pro, Palo Alto, USA).

4. pH Measurement

The variation of pH with immersion time in SBF was recorded after 1, 3, 7, and 14 days with a calibrated pH meter (Corning pH meter 340, USA).

5. SEM Analysis

The bioactivity of BG was confirmed by investigating the changing in morphology of its surfaces [59]. For this purpose, BG-5M and BG-5S were selected for SEM observation as a samples with the highest MTT and ALP activity among all synthesized MBG and S-BGs, respectively. Scanning electron microscope (SEM, Philips XL30, Netherland) was applied to evaluate the morphology of the formed HA on the surface of BG-5M and BG-5S after immersion in the SBF up to 14 days. Before examination, the surfaces of BGs were coated with a thin layer of gold (Au) by sputtering (EMITECH K450X, England) to prevent charges accumulation at its surface.

D. Biological Evaluation

1. Biocompatibility of the Synthesized BGs

For cytotoxicity evaluation, the proliferation of the MC3T3 cells on BGs was determined using the MTT (3-(4,5-dimethylthiazol-2-yl)-2,5-diphenyl-2H-tetrazolium bromide) assay [60]. For this purpose, cells were seeded on samples into a 96-well plate at a density of 6×10^3 cells per well with regular DMEM medium and incubated for 1, 3 and 7 days. At the end of time periods, the medium was removed and 100 μ L of 5 mg mL⁻¹ MTT solution (Sigma Aldrich) was added to each well. After incubation at 37 °C in a humidified atmosphere (95% air, 5% CO₂) for 72 h, the medium was removed and precipitated formazan was dissolved by adding dimethylsulfoxide (DMSO). The optical density (OD) value of the solution was read with multi-well microplate reader (EL 312e Biokinetics reader, Biotek Instruments) at a wavelength of 570 nm. The MC3T3-E1 cells growing in the absence of MBGs was used as control.

2. ALP Activity

The osteoblast activity was assessed by measuring the ALP production of MC3T3 cells as an early marker [61]. For this purpose, the cells were seeded on the BGs under the same culturing condition and at the end of each time period, the supernatant fluid was removed gently and the cell layer was rinsed well with PBS, followed by homogenizing with 1 mL Tris buffer and sonicating for 4 min on ice. Aliquots of 20 μ l were placed in equal volumes of 1ml of a p-nitrophenyl phosphate solution (pNPP, Sigma, 16 mmol.L⁻¹) and were incubated at 30 °C for up to 5 min.

3. Live-Dead Assay

The Live/Dead (viability/cytotoxicity) assay was used to qualitatively assess cell viability and to determine whether BGs were cytotoxic. For this purpose, MC3T3-E1 cells were cultured in the presence of BG-0 (control sample) and BG-5 (sample with the highest cell proliferation based on MTT results) for 7 days and then incubated with 4 mM ethidium homodimer-1 (EthD-1) and 2 mM calcein-acetoxymethyl ester (calcein-AM) at 37 °C in a humidified atmosphere of 5% CO₂-95% air for 15 min in dark. Then, cells were washed again with PBS to stop staining reaction. The stained cells (Live cells: green stain, Dead cells: red stain) were examined under fluorescence microscope (Olympus, USA) also representative

images were captured using a Zeiss AxioCam digital camera.

4. Actin Staining of MC3T3-E1 Cells

Dapi/Actin staining applied for visualizing the cytoskeleton and nuclei of MC3T3-E1 cells in presence of BG-0 (control sample), BG-5M and BG-5S (selected samples respectively for MBGs and S-BGs with the highest cell proliferation based on MTT results). For this purpose, the F-actins of MC3T3-E1 cells were stained in green with Alexa Fluor-594 phalloidin (Invitrogen), while the cells nuclei were stained in blue with 4,6-diamidine-2-phenylindole (DAPI) solution (Invitrogen). According to the manufacturer's procedure, after 1 and 7 days of incubation, cell-seeded BGs were rinsed with PBS twice and followed by fixation with 4% paraformaldehyde (Sigma-Aldrich, UK) solution for 30 min at room temperature. Afterward, samples soaked in 0.1% (v/v) Triton X-100 (Sigma)/PBS solution for 30 min. Finally, cells were washed three times with PBS and then were blocked in 1% (v/v) bovine serum albumin (BSA)/PBS solution for 1 h. The green fluorescence images of cytoskeleton and blue fluorescence images of nuclei of MC3T3-E1s were captured.

5. Antibacterial Evaluation

The individual effect of Mg and Sr substitution up to 10 mol.% in 58S-BG on antibacterial activities against MRSA bacteria was investigate. The bactericidal percentages were calculated according to the following formula by counting the final colony-forming units per milliliter (CFU mL⁻¹) [25], [26]. The procedure was illustrated in details in our previous work [18].

$$\text{Bactericidal fraction} = 1 - (\text{number of survived bacteria} / \text{number of total bacteria}).$$

E. Statistical analysis

The GraphPad Prism software package, version 3.0 (GraphPad Prism, USA) was used to statistical analysis. Each elemental analysis was performed with at least three samples and results were presented as means \pm standard deviations (SD). Moreover, P-value was considered statistically significant when *P<0.05 and P -values were more highly statistically significant when **p < 0.01, ***p < 0.001 and ****p < 0.0001.

III. RESULTS AND DISCUSSION

A. XRD Analysis

The XRD patterns of the BG-0 (control), M-BGs and S-BGs after 7 and 14 days of immersion are shown in Figs. 1 (a) and (b), respectively. As it seen in Fig. 1 (a), after 7 days of immersion, all the samples except BG-10M showed characteristic peak of crystalline HA according to the standard JCPDS (No. 09-432) [62] assign to (211) plane at 2 theta equal to 31.8°. Moreover, BG-0 showed another HA characteristic peak assign to (200) (plane) at 2 theta equal to 25.8° which confirmed substitution of Ca with Mg or Sr in 58S-BG resulted in a decrease in HA formation. This retarding effect was more pronounced in high amount of Mg (BG-10M)

compared to Sr (BG-10S). With increasing the immersion time to 14 days, the intensities of detected peaks increased due to the growth of the formed HA. Additionally, on day 14th, XRD patterns of all samples except BG-10M exhibited HA characteristic peak corresponding to (211) plane. Also, two more peaks corresponding to (112) and (300) planes were observed respectively at 2 theta equal 32.18° and 32.86° on XRD pattern of BG-0 which confirmed the HA maturity on BG-0 surfaces [63].

Previously, Ma et al. claimed that the higher substitution of MgO for CaO in SiO₂-CaO-MgO-P₂O₅ Bioglass, decreased its bioactivity due to blocking of active calcium phosphate growth sites by Mg²⁺ [49]. Roy et al. [64] reported the same reason for lower bioactivity in Na₂O-MgO-SiO₂ glass system. In addition, Hesaraki et al. [51] suggested that like Mg²⁺ [65], Sr²⁺ can also block the nucleation active sites of calcium phosphate nucleation active sites in sol-gel derived CaO-SrO-SiO₂-P₂O₅ BG and retarded the HA formation.

XRD results showed that both Mg/Ca and Sr/Ca substitution in BGs composition lowered the in vitro HA formation ability of the M-BGs and S-BGs. Moreover, high substitutions (BG-10M and BG-10S) had more retarding effect on HA formation with respect to moderate substitutions (BG-5M and BG-5S).

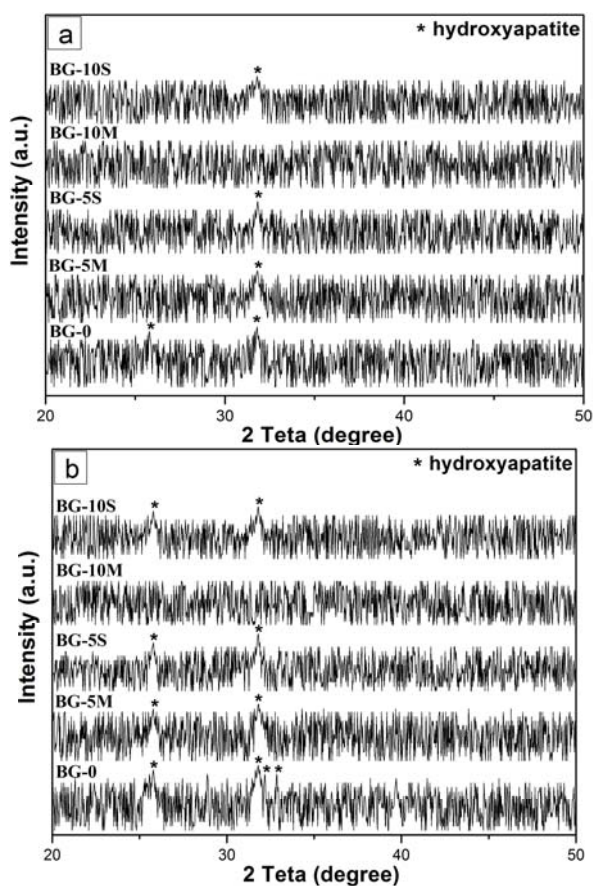


Fig. 1 The XRD patterns of BG-0, BG-5M, BG-5S, BG-10M and BG-10S after 7 and 14 days of soaking in SBF

B. Structural Groups

Figs. 2 (a) and (b) show the FTIR transmittance spectra of the synthesized BGs after 7 and 14 days of immersion in SBF, respectively. According to the literature [66–68], the main absorption bands attributed to the Si–O–Si bending, the Si–O symmetric stretching of bridging oxygen atoms between tetrahedrons, Si–O stretching of non-bridging oxygen atoms, Si–O–Si symmetric stretching and the Si–O–Si asymmetric stretching are located respectively at 470, 790, 922, 1066 and 1250 cm⁻¹. Additionally, the asymmetric vibrations of PO₄³⁻ are detected by band located at 570 and 603 cm⁻¹ which confirm the formation of calcium phosphate on BGs surface and also the absorption bands at 1455 cm⁻¹ and 870 cm⁻¹ are revealed due to C–O stretching in carbonate groups substituted for phosphate groups in HA lattice. Furthermore, the stretching mode of hydroxyl was determined by observing the band at 1651 cm⁻¹. Eventually, the stretching mode of OH group (hydroxyl) is determined by observing the band at 1651 cm⁻¹.

According to Fig. 2 (a), after 7 days of immersion, all the samples except BG-10M exhibited P–O and C–O bands which was in good agreement with XRD results (Fig. 1 (a)). With increasing the immersion period to 14 days, the intensities of observed peaks increased. But, still BG-10M did not show any phosphate or carbonate peaks.

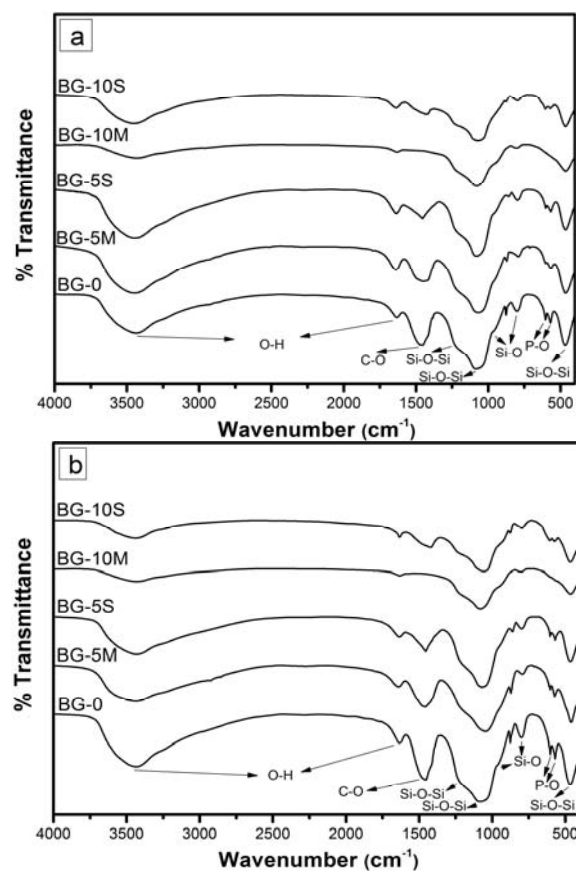


Fig. 2 FTIR spectra of BG-0, BG-5M, BG-5S, BG-10M and BG-10S after 7 and 14 days of soaking in SBF

By considering the appearance of P-O and C-O bands in FTIR spectra, it could be understood that in moderate amount of Mg and Sr (5 mol%), HA was formed on BG-5M and BG-5S surfaces after 7 days and more substitution of Mg and Sr up to 10 mol% retarded HA formation. Results indicated that Mg had more pronounced retarding effect in comparison with Sr. In the other words, BG-10M had the lowest bioactivity among all synthesized BGs.

C. Ion Chemistry of SBF Solution

In order to investigate the ions concentration variations after immersed in SBF for different time periods of 1, 3, 7 and 14 days, the reacted SBF was examined by ICP-AES. Figs. 3 (a)-(e) exhibits the variations of Ca, Si, P, Mg and Sr concentration in the SBF solution.

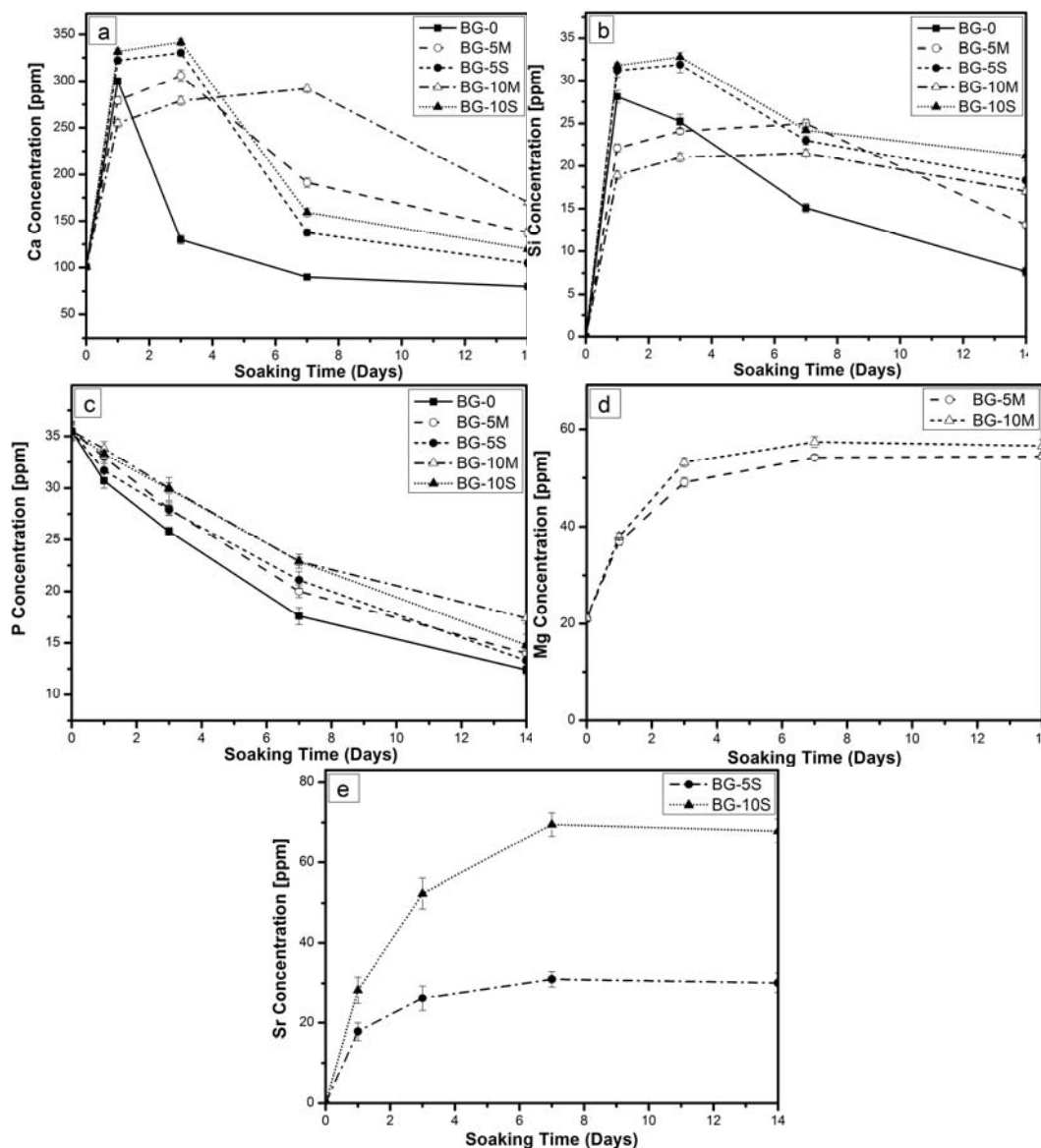


Fig. 3 Calcium (a), silicon (b), phosphorus (c), magnesium (d), strontium (e) ions concentrations in the SBF solution monitored over immersion time

According to the Fig. 3 (a), despite the primary concentration of Ca (approx. 100 ppm), Ca concentration $[Ca^{2+}]$ was increased instantly for all BGs. Additionally, after 1 day immersion, it seen that M-BGs and S-BGs had minimum and maximum Ca concentration, respectively. After 3 days immersion, $[Ca^{2+}]$ for BG-0 decreased while for other BGs increased gradually. Finally, after 3 days of immersion, $[Ca^{2+}]$ for BG-5, BG-5S and BG-10S were decreased. But,

BG-10M showed reverse trend.

The dissolution/precipitation of Ca^{2+} ions between BG surfaces and SBF during the crystallization of HA is monitored by change of Ca concentration [69], i.e. the decrease of $[Ca^{2+}]$ was indicative that the release of Ca^{2+} from BG surface into the SBF was lower than its precipitation from SBF on BGs surface. Fig. 3 (a) confirmed that BG-0 and BG-10M had respectively the highest and the lowest precipitation

rate of Ca^{2+} for calcium phosphate formation.

Fig. 3 (b) demonstrated that Si had similar trend like Ca and after immersion for 1 day, the Si concentrations were in the order S-BGs > BG-0 > M-BGs. Previously, Ma et al. reported the addition of Mg in BG resulted in a decrease in rate of magnesium-doped BG dissolution [59]. As SBF has no Si ions, the concentration of Si ions in SBF after immersion was investigated for BG's solubility. Sr^{2+} has larger ionic radius than Ca^{2+} (113 pm vs. 100 pm) and its substitution in BG composition results in a disruption of the BG network and causes network disorder in S-BG compared to BG-0. On the other hand, Mg^{2+} has smaller ionic radius than Ca^{2+} (72 pm vs. 100 pm) [70]. So, M-BG has more structural compactness (more ionic field strength) which prevents readily penetration of SBF inside the M-BGs structure. Table II shows the oxygen density values for BG-0, M-BGs and S-BGs. Therefore, according to Table II, the main reason for more solubility of S-BG compared to M-BG was its lower oxygen density due to less structure compactness.

TABLE II

THE OXYGEN DENSITY VALUES FOR SYNTHESIZED BGs

Glass	BG-0	BG-5M	BG-5S	BG-10M	BG-10S
Oxygen density	0.756±0.001	0.769±0.007	0.741±0.005	0.772±0.006	0.736±0.004

According to Fig. 3 (c), P concentration was decreased by increasing the immersion time up to 14 days for all BGs. Moreover, the rate of change in the P concentration revealed that an increase in the Mg and Sr contents resulted in a decrease the rate of HA precipitation.

Figs. 3 (d) and (e) showed the Mg and Sr release in the SBF were higher for BG-10M and BG-10S compared to BG-5M and BG-5S because of their more content in BG composition.

BGs exhibited a rapid increase in the Mg and Sr ion content until day 3rd and then reached a plateau on day 7th. The decreases in the dissolution rate of Mg and Sr in M-BGs and S-BGs by increasing the immersion time were due to the formation of silica rich and HA layers on the BG surfaces.

D. pH measurement

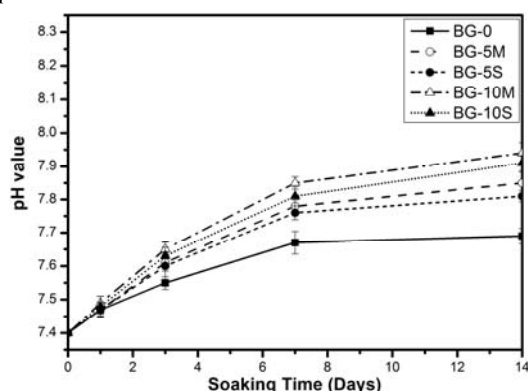


Fig. 4 pH variation of the SBF solution over immersion time up to 14 days

By considering the pH variations with immersion time (Fig. 4), it could be observed that M-BGs and S-BGs had higher pH

values in comparison with BG-0 due to the presence of alkaline earth elements. At first 7 days, the initial pH was rapidly increased from 7.4 to 7.81 and 7.85 for BG-10M and BG-10S, respectively. It could be explained by rapid ionic exchange between Ca^{2+} and alkaline earth elements from BGs and H^+ from SBF solution. Then, by precipitation and consumption of Ca ions for HA formation, the increasing rate of pH decreased and finally reached a plateau.

E. SEM Analysis

To study the morphology of the formed HA, the surfaces of the BG-5M and BG-5S (as selected samples of M-BGs and S-BGs, respectively with the highest bioactivity based on XRD and FTIR results) were observed under SEM after 14 days of immersion (Figs. 5 (a)-(d)). Fig. 5 (a) showed that the surface of BG-5M was fully covered by spherical calcium phosphate particles after 14 days of immersion, while rod-shaped calcium phosphate was formed on BG-5S (Fig. 5 (b)). The same rod-like HA was previously reported by Taherkhani et al. [55] in sol-gel derived 60% SiO_2 -36%(CaO/SrO)-4% P_2O_5 bioglass.

Based on SEM investigation, both BG-5M and BG-5S exhibited a promising bioactivity after 14 days of immersion in SBF.

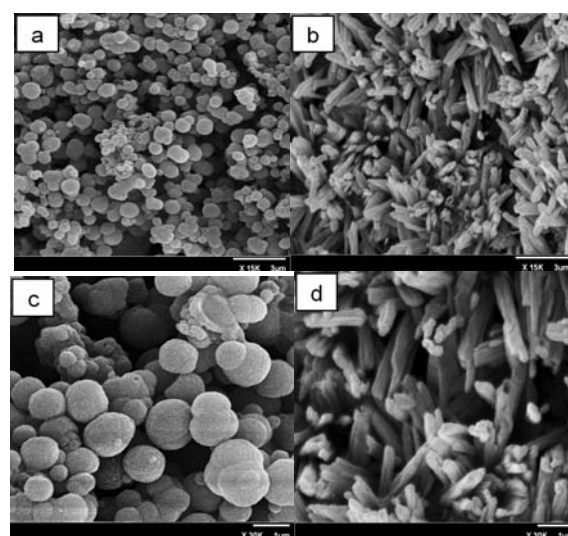


Fig. 5 SEM images of BG-5M (a and c (higher magnification)) and BG-5S (b and d (higher magnification)) after 14 days of immersion in the SBF solution

F. In vitro Biological Evaluation

1. MTT Evaluation

The MC3T3-E1 cells proliferation on BG-0, M-BG and S-BG for 1, 3, and 7 days was studied in order to assess the cytocompatibility of the synthesized BGs (Fig. 6). As it seen in Fig. 6, after first day of culture, BG-5M and BG-5S showed significant increase in cells proliferation compared with BG-0 (* $p < 0.05$). But, more substitution of $\text{Mg}^{2+}/\text{Ca}^{2+}$ and $\text{Sr}^{2+}/\text{Ca}^{2+}$ up to 10 mol% resulted in no significant increase (* $P > 0.05$). With increasing the culture time to 3 day, all the optical density (OD) values increased and the highest cell

proliferation attributed to the BG-5S in comparison with BG-0 (** $p < 0.01$). On 7th day of culture, both BG-5M and BG-5S exhibited the highest cell proliferation with respect to BG-0 (** $p < 0.01$), while BG-10M and BG-10S showed significant decrease (* $p < 0.05$) in optical density (OD) values. Previously, the effects of Mg and Sr in BGs on proliferation of cells were studied [71], [72]. Saboori et al. [71] claimed that 64% SiO₂-26% CaO-5% MgO-5% P₂O₅ (based on mol%) BG increased cell proliferation of human fetal osteoblast cells (hFOB 1.19). Moreover, the positive influence of Sr in moderate amount between 1% and 5% on proliferation and differentiation of osteoblastic ROS17/2.8 cells was reported by Qiu et al. [72]. MTT results suggested that substitution of 5 mol% Mg or Sr in BG 58S, significantly enhanced the MC3T3-E1 cells proliferation (** $p < 0.01$). Additionally, more substitution up to 10 mol% not only had no positive effect but also, significantly enhanced the MC3T3-E1 cells proliferation compared with BG-0 (* $p < 0.05$).

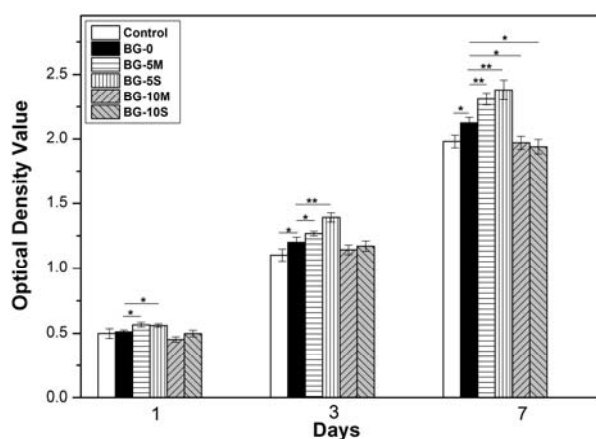


Fig. 6 Osteoblast-like cell line proliferation (MC3T3-E1), cultured on the synthesized BGs for 1, 3 and 7 days. (* $p < 0.05$ and ** $p < 0.01$)

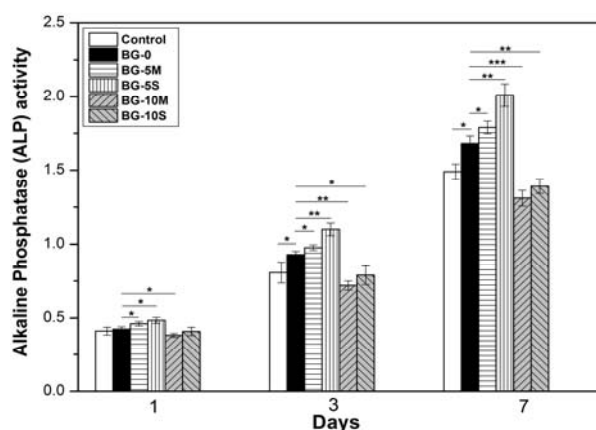


Fig. 7 ALP activities of osteoblast-like cell line (MC3T3-E1) cultured on synthesized BGs for 1, 3 and 7 days. (* $p < 0.05$ and ** $p < 0.01$)

2. Cell Activity

After 1, 3 and 7 days of culture, MC3T3-E1 cells differentiation was considered as ALP activity. Fig. 7

demonstrates the ALP activity of MC3T3-E1 cells treated with BG-0, M-BGs and S-BGs. As it seen in Fig. 7, after 1 day of culture, BG-5M significantly increased the MC3T3-E1 cells activity, while BG-10M showed the reverse effect. In other words, the substitution of Mg in moderate (5 mol %) and high (10 mol %) level led to significantly increase and decrease of MC3T3-E1 cells activities, respectively. Furthermore, the moderate substitution of Sr resulted in significant increase of MC3T3-E1 cells activity (* $p < 0.05$). But, more substitution (10 mol %) had no positive effect (* $p > 0.05$). By increasing the culture time, substitution of Sr in a moderate amount (5 mol %) caused higher ALP activity compared with Mg, i.e. BG-5S exhibited highly significant increase of ALP activity with respect to BG-5S.

The ALP activity study revealed that M-BG and S-BG with 5 mol% substitutions showed higher activity in comparison with 10 mol% substitutions and BG-5S had the highest ALP activity level among all synthesized BGs.

3. Live-Dead and Dapi/Actin Assays

In order to qualify study of the MC3T3-E1 cells viability in presence of Mg or Sr in BG composition, Live/Dead staining was performed for BG-0 (control), BG-5M and BG-5S after 1 and 7 days of culture (Fig. 8). After 1 day of culture, samples BG-5M (Fig. 8 (a)) and BG-5S (Fig. 8 (b)) showed better proliferation with relatively lower dead cells (red spot) compared with the control (Fig. 8 (a)) and also with increasing the culture time to 7 days, BG-5M and BG-5S showed more proliferation (almost confluence) with relatively lower dead cells in comparison to the BG-0.

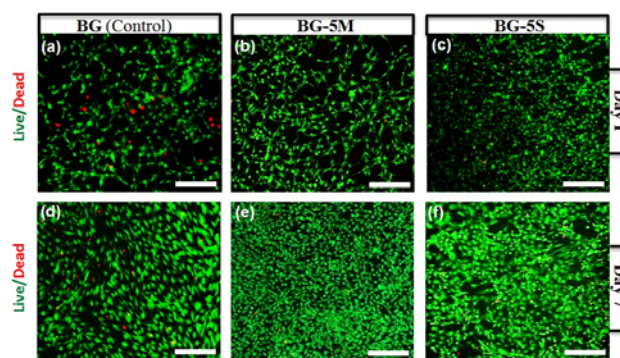


Fig. 8 Two-dimensional (2D) MC-3T3 cells cultured in presence of BG-0, BG-5M and BG-5S. Representative live/dead fluorescence images of MC-3T3 cells cultured on BG-0 (a, d), BG-5M (b, e) and BG-5S (c, f) after 1 and 7 days of culture respectively. Green fluorescent cells are alive and red fluorescent cells indicate dead cells. Scale bar represents 100 μ m in all images

Fig. 9 shows the F-actin-labeled cytoskeleton and nuclei of MC3T3-E1 treated with BG-0, BG-5M and BG-5S. By investigation the uniform spindle-like shape of MC3T3-E1 cells with random orientation, it could be understood that the mean number of DAPI-labelled nuclei treated with BG-5M and BG-5S was significantly increased in comparison to the control after 1 and 7 days of culture. The Dapi/Actin staining study was in a reasonable agreement with Live/dead results.

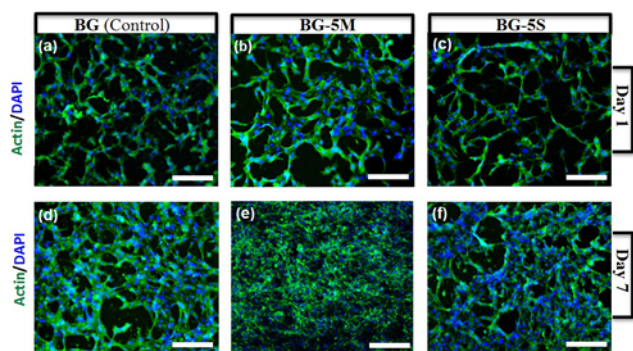


Fig. 9 Two-dimensional (2D) MC-3T3 cells cultured in presence of BG-0, BG-5 and BG-10. Representative ACTIN/DAPI fluorescence images of MC-3T3 cells cultured on BG-0 (a, d), BG-5M (b, e) and BG-5S (c, f) after 1 and 7 days of culture respectively. Cell filaments are stained by Actin (green) and nuclei stained by DAPI (blue). Scale bar represents 100 μm in all images.

Results indicated that the MC3T3-E1 cells were random orientation with relatively spindle-like shape. The same shapes of mesenchymal stem cells (rMSCs) were seen by He et al. [73] on the calcium carbonate ceramics. In addition, it was previously reported that biological response of the cells their metabolic activity were affected by ions dissolution from BGs [74] and pH change [75]. Previously, He et al. observed the spindle-like shape of rat bone mesenchymal stem cells (rMSCs) cultured on the calcium carbonate ceramics [73].

Live dead and Dapi/actin results revealed that the moderate concentration of Mg and Sr in culture medium resulted in a better cell proliferation in BG-5M and BG-5S, respectively.

It may be suggested that a moderate concentration of Mg and Sr in culture medium and pH values between 7.4 and 7.9 (Figs. 4 (d)-(e) and 5) led to a better cell proliferation. Consequently, the live and dead staining assay revealed that both BG-5M and BG-5S had the higher cell viability and proliferation compared to the control which was in a good agreement with MTT results (Fig. 6).

4. Antibacterial Studies

The effect of Mg and Sr in BG 58S composition on antibacterial activity of BG-0, M-BG and S-BG against MRSA bacteria is present in Fig. 10. It was seen that Mg had more pronounce effect than Sr. In other words, in the fixed concentration of 10 mg/ml BG in bacterial suspension, M-BGs showed significantly higher bactericidal efficiency against MRSA bacteria and the highest bactericidal efficiency was attributed to BG-5M since, BG-5M showed no significant increase compared to BG-0 ($P > 0.05$). Antibacterial investigation demonstrated that substitution of both magnesium (in moderate 5 mol% and high amount 10 mol%) and strontium (in high (10 mol %) resulted in a significant increase in bactericidal efficiency against MRSA. The exact mechanism for the bactericidal activity of BGs is not known [27], but some studies claimed that release of some ions such as Ca [27], P [27], Mg [76] and Sr [22] from BGs has responsible for the antibacterial property of BGs. Moreover, pH has another factor that may effect on antibacterial property

[25]. According to the ICP-OES and pH study, the release of Ca (Fig. 3 (a)), P (Fig. 3 (b)) and alkaline earth (Figs. 3 (e) and (f)) ions led to increasing the pH values which were probably the main reasons of M-BGs and S-BGs antibacterial effect.

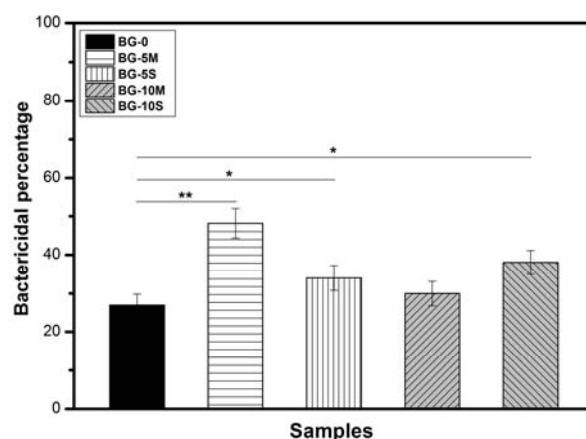


Fig. 10 The bactericidal percentages of 10 mg/mL of BG-0 (control), BG-5M, BG-5S, BG-10M and BG-10S. (* $p < 0.05$, ** $p < 0.01$, *** $p < 0.001$ and **** $p < 0.0001$)

Results showed that Mg exhibited dose-dependent antibacterial activity, while Sr had dose-independent behavior and BG-5 showed the highest antibacterial effect against MRSA bacteria among all synthesized BGs.

IV. CONCLUSIONS

A series of quaternary $60\text{SiO}_2-(36-x)\text{CaO}-4\text{P}_2\text{O}_5-(x)\text{yO}$ (where $x=0, 5$ and 10 ; $y= \text{Mg}$ or Sr) BGs were successfully synthesized through sol-gel method and the effects of Mg and Sr individual substitution with Ca in BG on in vitro HA formation, cytotoxicity, ALP activity and antibacterial efficiency were investigated. The in vitro bioactivity evaluation showed that the formation of HA on M-BGs and S-BGs was dose dependent and BG-5M and BG-5S had higher bioactivity compared with BG-10M and BG-10S due to less blocking of the active growth sites of calcium phosphate by alkaline earth ions. The ICP-OES results confirmed that replacement of Ca^{2+} with Mg^{2+} and Sr^{2+} caused a decrease and an increase in the solubility of M-BG and S-BG, respectively by changing the oxygen density. Additionally, both BG-5M and BG-5S significantly increase the MC3T3-E1 cells proliferation and activities with respect to the control ($*p < 0.05$).

Antibacterial study revealed that M-BG and S-BG had dose-dependent and dose-independent bactericidal effect against MRSA bacteria. Meanwhile, BG-5M exhibited the highest antibacterial efficiency among other BGs. Taken together, according to *in vitro* bioactivity, biological and antibacterial investigations, 5 mol% was presented as an optimal substitution of Mg/Ca and Sr/Ca in M-BGs and S-BGs; meanwhile, BG-5M is suggested as a promising multifunctional biomaterial in bone tissue regeneration engineering field.

REFERENCES

- [1] L. L. Hench, *J. Mater. Sci. Mater. Med.* 17 (2006) 967–978.
- [2] R. C. Bielby, I. S. Christodoulou, R. S. Pryce, W. J. P. Radford, L. L. Hench, J. M. Polak, *Tissue Eng.* 10 (2004) 1018–1026.
- [3] J. R. Jones, *Acta Biomater.* 9 (2013) 4457–4486.
- [4] M. N. Rahaman, D. E. Day, B. Sonny Bal, Q. Fu, S. B. Jung, L. F. Bonewald, A. P. Tomsia, *Acta Biomater.* 7 (2011) 2355–2373.
- [5] S. Kaya, M. Cresswell, A. R. Boccaccini, *Mater. Sci. Eng. C* 83 (2018) 99–107.
- [6] P. Sepulveda, J. R. Jones, L. L. Hench, *J. Biomed. Mater. Res.* 58 (2001) 734–740.
- [7] L. Treccani, T. Yvonne Klein, F. Meder, K. Pardun, K. Rezwan, *Acta Biomater.* 9 (2013) 7115–7150.
- [8] I. A. Silver, J. Deas, M. Ercińska, *Biomaterials* 22 (2001) 175–185.
- [9] S. Joughehdoust, S. Manafi, *Mater. Sci.* (2012).
- [10] P. Jha, K. Singh, *Ceram. Int.* 42 (2016) 436–444.
- [11] A. Moghanian, A. Sedghi, A. Ghorbanoghli, E. Salari, *Ceram. Int.* (2018).
- [12] A. Moghanian, S. Firoozi, M. Tahriri, *Ceram. Int.* 43 (2017).
- [13] S. Hesaraki, M. Alizadeh, H. Nazarian, D. Sharifi, *J. Mater. Sci. Mater. Med.* 21 (2010) 695–705.
- [14] L. Courthéoux, J. Lao, J.-M. Nedelec, E. Jallot, (2008).
- [15] C. Wu, Y. Zhou, M. Xu, P. Han, L. Chen, J. Chang, Y. Xiao, *Biomaterials* 34 (2013) 422–433.
- [16] J. J. Blaker, S. N. Nazhat, A. R. Boccaccini, *Biomaterials* 25 (2004) 1319–1329.
- [17] F. Sharifianjazi, N. Parvin, M. Tahriri, *Ceram. Int.* 43 (2017) 15214–15220.
- [18] A. Moghanian, S. Firoozi, M. Tahriri, *Ceram. Int.* 43 (2017) 12835–12843.
- [19] A. Moghanian, S. Firoozi, M. Tahriri, A. Sedghi, *Mater. Sci. Eng. C* 91 (2018) 349–360.
- [20] I. D. Xynos, A. J. Edgar, L. D. K. Buttery, L. L. Hench, J. M. Polak, *Biochem. Biophys. Res. Commun.* 276 (2000) 461–465.
- [21] J. R. Jones, L. M. Ehrenfried, P. Saravanapavan, L. L. Hench, *J. Mater. Sci. Mater. Med.* 17 (2006) 989–996.
- [22] J. Liu, S. C. F. Rawlinson, R. G. Hill, F. Fortune, *Dent. Mater.* 32 (2016) 412–422.
- [23] D. Campoccia, L. Montanaro, C. R. Arciola, *Biomaterials* 27 (2006) 2331–2339.
- [24] P. Stoor, E. Soderling, R. Grenman, *J. Biomed. Mater. Res.* 58 (2001) 113–120.
- [25] S. Hu, J. Chang, M. Liu, C. Ning, *J. Mater. Sci. Mater. Med.* 20 (2009) 281–286.
- [26] S. Hu, C. Ning, Y. Zhou, L. Chen, K. Lin, J. Chang, *J. Wuhan Univ. Technol. Sci. Ed.* 26 (2011) 226–230.
- [27] D. Khvostenko, T. J. Hilton, J. L. Ferracane, J. C. Mitchell, J. J. Kruzic, *Dent. Mater.* 32 (2016) 73–81.
- [28] M. C. Enright, D. A. Robinson, G. Randle, E. J. Feil, H. Grundmann, B. G. Spratt, *Proc. Natl. Acad. Sci. U. S. A.* 99 (2002) 7687–92.
- [29] I. Cacciotti, A. Bianco, M. Lombardi, L. Montanaro, *J. Eur. Ceram. Soc.* 29 (2009) 2969–2978.
- [30] H. Zreiqat, C. R. Howlett, A. Zannettino, P. Evans, G. Schulze-Tanzil, C. Knabe, M. Shakibaei, *J. Biomed. Mater. Res.* 62 (2002) 175–184.
- [31] R. K. Rude, H. E. Gruber, H. J. Norton, L. Y. Wei, A. Frausto, *J. Kilburn, Bone* 37 (2005) 211–219.
- [32] S. Pors Nielsen, *Bone* 35 (2004) 583–588.
- [33] S. Murphy, A. W. Wren, M. R. Towler, D. Boyd, *J. Mater. Sci. Mater. Med.* 21 (2010) 2827–2834.
- [34] P. J. Meunier, C. Roux, S. Ortolani, M. Diaz-Curiel, J. Compston, P. Marquis, C. Cormier, G. Isaia, J. Badurski, J. D. Wark, J. Collette, J. Y. Reginster, *Osteoporos. Int.* 20 (2009) 1663–1673.
- [35] J. Y. Reginster, E. Seeman, M. C. De Vernejoul, S. Adami, J. Compston, C. Phenekos, J. P. Devogelaer, M. D. Curiel, A. Sawicki, S. Goemaere, O. H. Sorensen, D. Felsenberg, P. J. Meunier, *J. Clin. Endocrinol. Metab.* 90 (2005) 2816–2822.
- [36] D. Bellucci, A. Sola, R. Salvatori, A. Anesi, L. Chiarini, V. Cannillo, *Mater. Sci. Eng. C* 72 (2017) 566–575.
- [37] S. J. Watts, R. G. Hill, M. D. O'Donnell, R. V. Law, *J. Non. Cryst. Solids* 356 (2010) 517–524.
- [38] M. Prabhu, K. Kavitha, P. Manivasakan, V. Rajendran, P. Kulandaivelu, *Ceram. Int.* 39 (2013) 1683–1694.
- [39] M. Erol, A. Özyuguran, Ö. Çelebicin, *Chem. Eng. Technol.* 33 (2010) 1066–1074.
- [40] F. Yang, D. Yang, J. Tu, Q. Zheng, L. Cai, L. Wang, *Stem Cells* 29 (2011) 981–991.
- [41] M. Saghiri, J. Orangi, A. Asaturian, *Dent. Mater.* (2017).
- [42] J. Wen, J. Li, H. Pan, W. Zhang, D. Zeng, L. Xu, Q. Wu, X. Zhang, X. Liu, X. Jiang, Y. Z. Zhang, G. Schlewitz, G. Szalay, M. Schumacher, M. Gelinsky, R. Schnettler, V. Alt, *J. Mater. Chem. B* 3 (2015) 4790–4804.
- [43] J. Du, Y. Xiang, *J. Non. Cryst. Solids* 358 (2012) 1059–1071.
- [44] W. Zhang, Y. Shen, H. Pan, K. Lin, X. Liu, B. W. Darvell, W. W. Lu, J. Chang, L. Deng, D. Wang, W. Huang, *Acta Biomater.* 7 (2011) 800–808.
- [45] Y. Li, A. Matinmanesh, D. J. Curran, E. H. Schemitsch, P. Zalzal, M. Papini, A. W. Wren, M. R. Towler, *J. Non. Cryst. Solids* 458 (2017) 69–75.
- [46] J. Lao, E. Jallot, J.-M. Nedelec, *Chem. Mater.* 20 (2008) 4969–4973.
- [47] D. Sriranganathan, N. Kanwal, K. A. Hing, R. G. Hill, *J. Mater. Sci. Mater. Med.* 27 (2016) 39.
- [48] J. Pérez-Pariente, A. F. Balas, M. Vallet-Regí*, *Chem. Mater* 12 (2000) 750–755.
- [49] J. Ma, C. Z. Chen, D. G. Wang, Y. Jiao, J. Z. Shi, *Colloids Surfaces B Biointerfaces* 81 (2010) 87–95.
- [50] E. Dietrich, H. Oudadesse, *J. Biomed.* 88 (2009) 1087–1096.
- [51] S. Hesaraki, M. Gholami, S. Vazehrad, S. Shahrabi, *Mater. Sci. Eng. C* 30 (2010) 383–390.
- [52] A. Goel, R. R. Rajagopal, J. M. F. Ferreira, *Acta Biomater.* 7 (2011) 4071–4080.
- [53] J. Lao, J. M. Nedelec, E. Jallot, Y. Tsouderos, P. Deloffre, M. Hott, P. J. Marie, P. D. Delmas, C. Christiansen, H. Seznec, R. Rizzoli, H. K. Genant, J. Y. Reginster, *J. Mater. Chem.* 19 (2009) 2940.
- [54] A. Hoppe, B. Sarker, R. Detsch, N. Hild, D. Mohn, W. J. Stark, A. R. Boccaccini, *J. Non. Cryst. Solids* 387 (2014) 41–46.
- [55] S. Taherkhani, F. Moztarzadeh, *J. Sol-Gel Sci. Technol.* 78 (2016) 539–549.
- [56] J. S. Moya, A. P. Tomsia, A. Pazo, C. Santos, F. Guitin, *J. Mater. Sci. Mater. Med.* 5 (1994) 529–532.
- [57] J. Christie, N. de Leeuw, *J. Mater. Sci.* (2017).
- [58] T. Kokubo, H. Kushitani, S. Sakka, T. Kitsugi, T. Yamamuro, *J. Biomed. Mater. Res.* 24 (1990) 721–734.
- [59] J. Ma, C. Z. Chen, D. G. Wang, X. Shao, C. Z. Wang, H. M. Zhang, *Ceram. Int.* 38 (2012) 6677–6684.
- [60] K. Zheng, S. Yang, J. Wang, C. Rüssel, C. Liu, W. Liang, *J. Non. Cryst. Solids* 358 (2012) 387–391.
- [61] S. Ni, J. Chang, L. Chou, *J. Biomed. Mater. Res. Part A* 76A (2006) 196–205.
- [62] Z. Zhong, J. Qin, J. Ma, *Ceram. Int.* 41 (2015) 8878–8884.
- [63] S. Shahrabi, S. Hesaraki, S. Moemeni, M. Khorami, *Ceram. Int.* 37 (2011) 2737–2746.
- [64] D. Roy, *J. Phys. Chem. Solids* 68 (2007) 2321–2325.
- [65] Z. Amjad, P. Koutsoukos, G. Nancollas, *J. Colloid Interface Sci.* 101 (1984) 250–256.
- [66] X. Wu, G. Meng, S. Wang, F. Wu, W. Huang, Z. Gu, *Mater. Sci. Eng. C* 52 (2015) 242–250.
- [67] X. Zhang, Y. Wu, S. He, D. Yang, *Surf. Coatings Technol.* 201 (2007) 6051–6058.
- [68] M. Mozafari, M. Rabiee, M. Azami, S. Maleknia, *Appl. Surf. Sci.* 257 (2010) 1740–1749.
- [69] L. L. Hench, J. Wilson, *An Introduction to Bioceramics*, World Scientific, 1993.
- [70] G. S. Lázaro, S. C. Santos, C. X. Resende, E. A. dos Santos, *J. Non. Cryst. Solids* 386 (2014) 19–28.
- [71] A. Saboori, M. Rabiee, F. Moztarzadeh, M. Sheikhi, M. Tahriri, M. Karimi, *Mater. Sci. Eng. C* 29 (2009) 335–340.
- [72] K. Qiu, X. J. Zhao, C. X. Wan, C. S. Zhao, Y. W. Chen, *Biomaterials* 27 (2006) 1277–1286.
- [73] F. He, J. Zhang, F. Yang, J. Zhu, X. Tian, X. Chen, *Mater. Sci. Eng. C* 50 (2015) 257–265.
- [74] P. Valerio, M. M. Pereira, A. M. Goes, M. F. Leite, *Biomaterials* 25 (2004) 2941–2948.
- [75] W. K. Ramp, L. G. Lenz, K. K. Kaysinger, *Bone Miner.* 24 (1994) 59–73.
- [76] Robinson D Griffith R Shechtman D Evans R Conzemius M, *Acta Biomater.* 6 (2010) 1869–1877.